



**HAL**  
open science

# Comparing TiO<sub>2</sub> photocatalysis and UV-C radiation for inactivation and mutant formation of *Salmonella typhimurium* TA102

Antonino Fiorentino, Luigi Rizzo, H el ene Guilloteau, Xavier Bellanger,  
Christophe Merlin

► **To cite this version:**

Antonino Fiorentino, Luigi Rizzo, H el ene Guilloteau, Xavier Bellanger, Christophe Merlin. Comparing TiO<sub>2</sub> photocatalysis and UV-C radiation for inactivation and mutant formation of *Salmonella typhimurium* TA102. *Environmental Science and Pollution Research*, Springer Verlag, 2017, 24 (2), pp.1871 - 1879. 10.1007/s11356-016-7981-6 . hal-01767777

**HAL Id: hal-01767777**

**<https://hal.univ-lorraine.fr/hal-01767777>**

Submitted on 5 Oct 2021

**HAL** is a multi-disciplinary open access archive for the deposit and dissemination of scientific research documents, whether they are published or not. The documents may come from teaching and research institutions in France or abroad, or from public or private research centers.

L'archive ouverte pluridisciplinaire **HAL**, est destin ee au d ep ot et  a la diffusion de documents scientifiques de niveau recherche, publi es ou non,  emanant des  tablissements d'enseignement et de recherche fran ais ou  trangers, des laboratoires publics ou priv es.

1 **Comparing TiO<sub>2</sub> photocatalysis and UV-C radiation for inactivation and mutants formation of**

2 ***Salmonella typhimurium* TA102**

3 Antonino Fiorentino<sup>1</sup>, Luigi Rizzo<sup>1\*</sup>, H el ene Guilloteau<sup>2,3</sup>, Xavier Bellanger<sup>2,3</sup>, Christophe Merlin<sup>2,3</sup>.

4 <sup>1</sup>Department of Civil Engineering, University of Salerno, Via Giovanni Paolo II, 132, 84084 Fisciano (SA),  
5 Italy

6 <sup>2</sup>CNRS, Laboratoire de Chimie Physique et Microbiologie pour l'Environnement (LCPME), UMR 7564,  
7 Institut Jean Barriol, 15 Avenue du Charmois, 54500 Vandoeuvre-l es-Nancy, France

8 <sup>3</sup>Universit e de Lorraine, LCPME, UMR 7564, 15 Avenue du Charmois, 54500 Vandoeuvre-l es-Nancy,  
9 France

10 \*Corresponding author: Tel.: +39 089 969334; fax: +39 089 969620

11 E-mail address: l.rizzo@unisa.it

12

13

14 **Abstract**

15 Salmonellosis is one of the most common causes of foodborne bacterial human disease worldwide and the  
16 emergence of multidrug resistant (MDR) strains of *Salmonella enterica* serovar Typhimurium (*S.*  
17 *typhimurium*) was associated to the incidence of invasive salmonellosis. The objective of the present work  
18 was to investigate the effects of the TiO<sub>2</sub> photocatalysis process in terms of both bacteria inactivation and the  
19 emergence of mutants, on *S. typhimurium* TA102 water suspensions. The TiO<sub>2</sub> photocatalysis was compared  
20 with a conventional disinfection process *i.e.* UV-C radiation. In spite of the faster bacterial inactivation  
21 obtained in UV-C disinfection experiments (45, 15 and 10 min for total inactivation for initial cell density 10<sup>9</sup>,  
22 10<sup>8</sup> and 10<sup>7</sup> CFU mL<sup>-1</sup>, respectively), photocatalytic disinfection (60, 30 and 15 min) was more energy efficient  
23 because of a lower energy requirement (2 - 20 mWs cm<sup>-2</sup>) compared to the UV-C disinfection process (5 - 30  
24 mWs cm<sup>-2</sup>). During the photocatalytic experiments, the mutation frequency increased up to 1648 fold  
25 compared to background level for a 10<sup>8</sup> CFU mL<sup>-1</sup> initial bacterial density, and mutants were inactivated after  
26 1 - 10 min treatment, depending on initial bacterial cell density. In UV-C disinfection experiments, the  
27 mutation frequency increased up to 2181 fold for a 10<sup>8</sup> CFU mL<sup>-1</sup> initial bacterial cell density, and UV-C doses  
28 in the range 0.5 - 4.8 mWs cm<sup>-2</sup> were necessary to decrease mutation frequency. In conclusion, both  
29 disinfection processes were effective in the inactivation of *S. typhimurium* cells and mutants release into the  
30 environment can be avoided if cells are effectively inactivated.

31

32 Keywords: advanced oxidation processes, Ames test, mutagenicity, *Salmonella typhimurium*, water  
33 disinfection.

34

36 Salmonellosis is one of the most common causes of foodborne bacterial human disease worldwide and a  
37 significant increase in the number of *Salmonella* infections has been observed in many countries over the past  
38 decade (Rahmani et al. 2013). Specifically, *Salmonella* spp. results in approximately 93.8 million cases of  
39 gastroenteritis annually worldwide, leading to 155,000 deaths each year (Majowicz et al. 2010). The genus  
40 *Salmonella* comprises two species *S. bongori* and *S. enterica*, the latter one being in turn divided in six sub-  
41 species that cover more than 2550 serovars according to their O and H antigens. Among them, *S. enterica*  
42 serovar Typhimurium, is a primary enteric pathogen mainly associated to human and other warm-blooded  
43 vertebrates (Popoff 2001, Fàbrega and Vila 2013). In the last years, a close association was reported between  
44 the emergence of multidrug resistant (MDR) strains of *Salmonella* and the incidence of invasive salmonellosis  
45 (Gordon et al. 2008). The increased frequency of MDR *Salmonella* strains in human infections and the ensuing  
46 consequences it has on a health perspective (Oubrim et al. 2012; Rahman et al. 2014), brings to light the  
47 possible role of fecally contaminated waters in the spread of MDR *Salmonella* (Levantesi et al. 2012).

48 Food and water still play the main roles in the transmission of *Salmonella*. *Salmonellae* are excreted through  
49 animal and human feces into the environment and are frequently found in aqueous matrices. In particular, they  
50 typically occur in large numbers in raw sewage (Oubrim et al. 2012) and can still persist in wastewater  
51 effluents (Masarikova et al. 2016) even after a disinfection process (Wéry et al. 2008). A study indicated that  
52 80% of wastewater samples used for irrigation was positive for *Salmonella* (Nutt et al. 2003). Moreover, it  
53 has been detected in various types of natural waters such as rivers, lakes, coastal waters, as well as  
54 contaminated ground water (Polo et al. 1999; Martinez-Urtaza et al. 2004; Haley et al. 2009; Levantesi et al.  
55 2010).

56 Different studies have investigated the inactivation of *Salmonella* strains by disinfection processes in water  
57 and wastewater. In particular, Koivunen and Heinonen-Tanski (2005) evaluated the effect of different  
58 disinfection processes on *Salmonella* strains in synthetic wastewater where the treatment with peracetic acid  
59 and UV radiation has been shown to be faster than UV radiation alone and chlorine processes for the  
60 inactivation of *Salmonella enteritidis*. In some instance, *Salmonella* has been found to be more resistant to  
61 disinfection processes than others bacterial indicators (Berney et al. 2006; Rincon and Pulgarin 2007, Sciacca  
62 et al. 2011; Li et al. 2012). On the other hand, conventional disinfection by either chlorination or UV radiation  
63 may not be effective enough in controlling the spread of pathogens including ~~resistant microorganisms and~~

64 particularly antibiotic resistance microorganisms (Rizzo et al. 2013), therefore alternative disinfection  
65 methods should be investigated. Advanced oxidation processes (AOPs) (e.g., Fenton, photo-Fenton, TiO<sub>2</sub>  
66 photocatalysis, UV/O<sub>3</sub>, UV/H<sub>2</sub>O<sub>2</sub> etc.) have been found effective in the removal of a wide range of  
67 contaminants (Rizzo 2011). Among AOPs, TiO<sub>2</sub> photocatalysis is a promising water disinfection option,  
68 because of its capacity to inactivate a wide range of pathogens in water (Dunlop et al. 2011; Polo-López et al.  
69 2014; Rizzo et al. 2014a); however, to the best of our knowledge, the effectiveness of TiO<sub>2</sub> photocatalysis on  
70 the inactivation of selected *Salmonella* strains and/or its possible effect in terms of mutagenicity has not been  
71 investigated so far. Indeed, if the inactivation of microbial indicators during treatment/disinfection processes  
72 is well documented, specific process-induced mutagenicity is generally occulted, apart from demonstrating  
73 the production of genotoxic by-products. Yet, in *Salmonella* as for other organisms, gene mutations can confer  
74 resistance to antimicrobial by altering the corresponding protein target or by altering the substrate specificity  
75 of existing antimicrobial degrading enzymes (Michael et al. 2006). Thus, beyond bacterial inactivation,  
76 considering process-induced mutagenicity might prove to be of prime importance for a better control of  
77 antibiotic resistance pathogens in the released effluents. In fact, antibiotic resistances can be acquired either  
78 through gene transfer or by mutation of the target gene. If the effects of various treatment strategies on the  
79 persistence of resistance genes/bacteria start now to be relatively well documented, the effects of such  
80 treatments on the emergence (mutation) and dissemination (transfer) of antibiotic resistance genes remains  
81 scarce nay inexistent, and needs further consideration (Sharma et al 2016).

82 The objective of the present work was to investigate the effects of the TiO<sub>2</sub> photocatalysis process in terms of  
83 inactivation and mutagenicity on a model microorganism. *Salmonella* was chosen as target/model organism  
84 (its genus belongs to the *Enterobacteriaceae*, the same family as *Escherichia*, which includes the species *E.*  
85 *coli*) because of (i) its spread in aqueous matrices (particularly in natural water and wastewater), (ii) the related  
86 concern for human health (it can cause illnesses such as typhoid fever and paratyphoid fever) and (iii) its role  
87 in antibiotic resistance spread. Moreover, the effect of TiO<sub>2</sub> photocatalysis on the inactivation and  
88 mutagenicity of *Salmonella* was compared with a conventional disinfection process *i.e.* UV-C disinfection.

## 89 **2. Material and methods**

### 90 **2.1 Bacterial strain and media**

91 *Salmonella enterica* serovar Typhimurium strain TA102 was used as tester strain for general mutagenicity  
92 testing according to Maron and Ames (1983). Strain TA102 has been extensively used and reported under its  
93 former species name “*Salmonella typhimurium*” and will be reported as such in this manuscript to avoid  
94 unnecessary confusion. Strain TA102 exhibits a requirement for histidine and therefore cannot grow on  
95 minimal medium unless the *his428* mutation, carried on its plasmid pAQ1, mutates back to a prototrophic  
96 form. *S. typhimurium* TA102 was routinely cultured at 37°C on Vogel-Bonner minimal medium supplemented  
97 with D-Glucose, D-Biotin and L-Histidine (Maron and Ames 1983). For isolation of His<sup>+</sup> revertants, the  
98 histidine supplement was omitted from the medium. Strain *S. typhimurium* TA102 was selected among a  
99 variety of other *Salmonella* tester strains because of its noticeable sensitivity to numerous mutagenic agents,  
100 including UV, that are otherwise poorly detected by alternative tester strains (Maron and Ames 1983).  
101 TA102 bacteria were unfrozen and revived by streaking on Vogel-Bonner agar plate supplemented with  
102 Glucose and Histidine and incubated at 37 °C for 48 h. A single colony from the plate was inoculated into 10  
103 mL sterile lysogeny broth (LB, Sigma-Aldrich, USA) and incubated at 30°C for 18 h under agitation (160  
104 rpm) in a rotating shaker to obtain a stationary phase culture. Cells were washed twice by alternating  
105 centrifugations at 5000 rpm for 2 min and pellets re-suspensions in 10 mM MgSO<sub>4</sub>. The final volumes were  
106 adjusted to obtain cell concentrations at either 10<sup>9</sup>, 10<sup>8</sup> or 10<sup>7</sup> CFU mL<sup>-1</sup>; these suspensions were prepared  
107 independently and then used in independent disinfection experiments.

108

## 109 **2.2 TiO<sub>2</sub> photocatalysis tests**

110 Photocatalytic tests were carried out in a 2.2 L cylindrical glass reactor (13.0 cm in diameter) filled in with  
111 the 400 mL of sample. The thickness of liquid was constant and equal to the liquid depth (3 cm). The reactor  
112 was placed in a water bath to control the temperature at 30°C during the experiments. The aqueous suspension  
113 in the reactor was stirred continuously. A wide spectrum 250 W lamp (Procomat, Italy) with a peak of light  
114 intensity in the UV-A range of 0.012 mW cm<sup>-2</sup> at 350 nm was used as light source. The lamp was placed  
115 horizontally, 40 cm above the surface of the water. Degussa P25 TiO<sub>2</sub> was used as slurry as received from the  
116 manufacturer to perform heterogeneous photocatalytic experiments. They were carried out at concentration of  
117 100 mg L<sup>-1</sup> according to previously set conditions (Rizzo et al. 2014b). Finally, control tests with TiO<sub>2</sub> under  
118 dark conditions and UV irradiation alone were carried out in order to distinguish their respective contribution

119 to *S. typhimurium* TA102 inactivation and stress-induced mutagenicity compared to the photocatalytic  
120 process.

121

### 122 **2.3 UV-C disinfection tests**

123 UV-C experiments were carried out in 40 mL glass Petri dishes (diameter: 90 mm) filled in with 25 mL of  
124 sample. Petri dishes were gently stirred throughout the exposure time under a collimating apparatus (Simonet  
125 and Gantzer, 2006) equipped with a low-pressure mercury vapor lamp (10-W Slimline germicidal lamp,  
126 ozone-free Ster-L-Ray G12T6L; Atlantic UV Corporation) emitting monochromatic (253.7-nm) UV light.  
127 The irradiance at the center of the beam at the water surface was about 0.008 mW cm<sup>-2</sup>, and was delivered by  
128 a UV tube positioned horizontally, 20 cm above the surface of the water. Different UV-C doses were achieved  
129 by varying the exposure time

130

### 131 **2.4 Bacterial count and mutation frequencies**

132 Bacterial cells exposed to UV-C and TiO<sub>2</sub> photocatalysis treatment were recovered, serially diluted in 10 mM  
133 MgSO<sub>4</sub>, and spread in triplicate on minimal glucose agar with and without histidine. Plates were incubated at  
134 37°C for 48-72h. Each sample was analyzed in triplicate. Mutation frequencies were obtained as ratios  
135 between the number of revertants (counts on plates without histidine) and the total bacterial cell counts (on  
136 medium with histidine).

137

### 138 **2.5 Statistical analysis**

139 The correlations between the bacterial mortality ( $\log(N/N_0)$ ) and the duration of the treatments, or the doses  
140 received, were assessed using the Pearson's test. Then, regression data analyses were performed on log-  
141 transformed data:  $\log(N/N_0)$  for the total cell counts and  $\log(F/F_0)$  for the frequencies of mutation. The effects  
142 of both the treatment and the initial bacterial cell load were analyzed using a Fisher F-test and a Student T-  
143 test. The "Fisher F-test" was used to test data for homogeneity of variances. Thereafter, once homogeneity  
144 was verified, a "Student T-test" was further used to compare the trends (slopes) of linear regressions. A  
145 statistical difference revealed by a Student T-test, combined to the comparison of regression trendlines (slopes)

146 allowed determining whether a given treatment or condition had stronger effects than another one. Statistical  
147 correlations and statistical comparisons are presented in supplementary material.

148

### 149 **3. Results and discussion**

#### 150 **3.1 TiO<sub>2</sub> photocatalytic tests**

##### 151 *3.1.1 Control tests*

152 Photocatalytic tests were carried out by using a wide spectrum lamp with the main emission in UV-A  
153 wavelength range (400-315 nm) and TiO<sub>2</sub> as photocatalyst. Therefore, control tests were carried out using  
154 UV-A radiation and TiO<sub>2</sub> as stand-alone processes in order to evaluate the effective contribution of  
155 photocatalytic process (UV/TiO<sub>2</sub>) on both the inactivation of strain TA102 and the induction of His<sup>+</sup> revertant  
156 mutants.

157 TiO<sub>2</sub> control experiments were carried out in the dark and did not result in any significant change neither in  
158 the initial bacterial density and nor the mutants count (2h treatment; data not shown). UV-A control tests were  
159 carried out up over time to 15, 30 and 60 min irradiation time with initial cell suspension density of 10<sup>7</sup>, 10<sup>8</sup>  
160 and 10<sup>9</sup> CFU mL<sup>-1</sup>, respectively, according to the respective minimum treatment time necessary to achieve  
161 total *S. typhimurium* TA102 inactivation by the corresponding UV/TiO<sub>2</sub> process. As shown in Figure 1 and  
162 Supplementary section 3, the UV-A control tests resulted in a moderate (but statistically significant) cell  
163 inactivation and weak changes in mutation frequency over the course of the UV-A exposure time

164

165

Figure 1

166

167 The bacteria inactivation clearly appears exposure time dependent, it did not seem to be significantly  
168 influenced by initial cell load as for a given time of UV-A exposure a similar cell count reduction is observed  
169 (ca. 1 log reduction for a 15 min exposure). On a statistical point of view, the decreasing trend in viable cell  
170 counts correlates with the exposure time but the absence of homogenous variances does not allow drawing  
171 any conclusion regarding a possible effects of the initial cell load (Supplementary sections 2 and 3). The  
172 evolution of the His<sup>+</sup> mutant counts appear to decrease at a slower pace compared to the total viable count,  
173 with 0.5 log units decrease after 15 min to 2.2 log units decrease after 60 min treatment time (Figure 1a). This



174 may indicate that an increase of the mutation frequency, therefore producing more His<sup>+</sup> mutants, could  
175 partially compensate the inactivation of the His<sup>+</sup> subpopulation. This seems to be particularly true for the 10<sup>9</sup>  
176 CFU mL<sup>-1</sup> initial cell density suspension, where a 231 fold increase of the mutation frequency was reached  
177 after 60 min of UV-A exposure. Nevertheless, when comparing the different evolution of the mutation  
178 frequencies (log F/F<sub>0</sub>) as a function of the treatment dose (exposure time), no statistical difference was  
179 observed between the different initial cell loads (Supplementary Fig. S2, Table S3).

180 The inactivation of *S. typhimurium* TA102 can be explained through the damage caused by UV-A radiation  
181 following its absorption by cellular components called intracellular chromophores. Light absorption through  
182 chromophores contributes to the generation of reactive oxygen species (ROS). According to McGuigan et al.  
183 (2012), the UV-A wavelengths bordering on visible light are not sufficiently energetic to alter DNA directly.  
184 Nevertheless, UV-A play an important role in promoting the formation of intracellular ROS (singlet oxygen,  
185 superoxide, hydrogen peroxide, and hydroxyl radical), which can in turn damage DNA.

186

### 187 3.1.2 *S. typhimurium* TA102 inactivation by TiO<sub>2</sub> photocatalysis

188 The results of *S. typhimurium* TA102 inactivation by TiO<sub>2</sub> photocatalysis are plotted as function of irradiation  
189 time in Figure 2.

190

### 191 Figure 2

192

193 The initial bacterial density strongly affected the inactivation rate by TiO<sub>2</sub> photocatalysis (Fig. 2;  
194 Supplementary section 4). The complete bacterial inactivation was achieved after 60, 30 and 15 min of  
195 irradiation for initial bacterial densities of 10<sup>9</sup>, 10<sup>8</sup> and 10<sup>7</sup> CFU mL<sup>-1</sup>, respectively. Compared to control test  
196 with UV-A radiation alone (Fig.1), TiO<sub>2</sub> photocatalytic process was found to be undoubtedly more effective,  
197 which was further demonstrated by a Student comparison T-tests on both series of data (Supplementary section  
198 6). Cho et al. (2004) evaluated the correlation between hydroxyl radicals (<sup>•</sup>OH) and *E. coli* inactivation rates  
199 under UV/TiO<sub>2</sub> treatment. The concentration of <sup>•</sup>OH during photocatalytic treatment was quantified by  
200 measuring p-chlorobenzoic acid (a probe compound) degradation rate. The results demonstrated an excellent  
201 linear correlation between <sup>•</sup>OH and the rate of *E. coli* inactivation, which indicates that the <sup>•</sup>OH radical is the  
202 primary oxidant species responsible for inactivating *E. coli* in the UV/TiO<sub>2</sub> process. The inactivation of *S.*  
203 *typhimurium* TA102 by photocatalysis with UV-A lamp in combination with TiO<sub>2</sub> at concentration of 0.5 g L<sup>-1</sup>

204 <sup>1</sup> was studied by Long et al. (2014). Three different initial cell loads were investigated:  $10^7$ ,  $10^6$  and  $10^5$  CFU  
205  $\text{mL}^{-1}$ , and a complete inactivation was reached after 180, 70 and 60 min respectively. Slower inactivation rates,  
206 as might be expected, were obtained with only the UV-A lamp. A similar study, with the inactivation of  
207 *Salmonella enteritidis* (initial bacterial density of  $10^8$  CFU  $\text{mL}^{-1}$ ) by UV-A lamp and  $\text{TiO}_2$  at concentration of  
208  $1.0 \text{ g L}^{-1}$  was carried out by Robertson et al. (2005). A decrease of 5 log units was reached after 120 min of  
209 treatment, however, quite surprisingly, little difference was observed in experiments without catalyst and only  
210 with UV-A lamp. In our previous experiments, the effect of  $\text{TiO}_2$ /sunlight experiment on antibiotic resistant  
211 *Escherichia coli* strains was investigated by using the same experimental set up (2.2 L cylindrical glass reactor  
212 and 250 W lamp) and a total inactivation was achieved after 60 min, with  $100 \text{ mg L}^{-1}$  of  $\text{TiO}_2$  and an initial  
213 bacterial load of  $10^6$  CFU  $\text{mL}^{-1}$  (Rizzo et al. 2014b). Wang et al. (2014) also reported that the rate of bacterial  
214 inactivation, or real antimicrobial activity by  $\text{TiO}_2$ , depends on the initial bacterial concentration. In the present  
215 study, we also found that the inactivation rate of strain TA102 was exposure time-dependent and statistically  
216 stronger as the initial cell load decrease (Supplementary section 4). Possibly, when the initial bacteria  
217 population is too high, there is a bigger buffering capacity for the hydroxyl radicals, which is not only due to  
218 the large amount of cells but also from the mineralization products in the reaction process. In 2011, Foster et  
219 al. proposed a killing mechanism where hydroxyl radicals progressively damage the cell surface structures  
220 leading to the release of intracellular material/molecules that can in turn be undergo further degradation up to  
221 a complete mineralization. From this it can then be assumed that the released intracellular components here  
222 seen as intermediate products of photocatalysis, have a protective effect on live bacteria as they compete with  
223 live cells for interacting with hydroxyl radicals, and thus contribute to the loss of antibacterial activity. ~~In our~~  
224 ~~previous experiments, the effect of  $\text{TiO}_2$ /sunlight experiment on antibiotic resistant *Escherichia coli* strains~~  
225 ~~was investigated by using the same experimental set up (2.2 L cylindrical glass reactor and 250 W lamp) and~~  
226 ~~a total inactivation was achieved after 60 min, with  $100 \text{ mg L}^{-1}$  of  $\text{TiO}_2$  and an initial bacterial load of  $10^6$  CFU~~  
227  ~~$\text{mL}^{-1}$  (Rizzo et al. 2014b).~~

228 In spite of the debate over which process lead to death of an organism exposed to photocatalytic action, most  
229 of the experimental evidences show that the destruction of the cell membrane is an important issue for  
230 inactivation (Dalrymple et al. 2010). The mechanism for bacterial destruction by  $\text{TiO}_2$  photocatalysis has been  
231 proposed to occur via attack by  $\cdot\text{OH}$  generated on the photocatalyst surface and the mode of microbial  
232 destruction suggest that initial target for photocatalytic attack is the bacterial cell wall. Gram-negative cell  
233 wall includes a thin peptidoglycan layer, and an external membrane made of lipopolysaccharide (LPS) and

234 phospholipid. In gram-negative bacteria, peptidoglycan layer makes up only about 10% of the cell wall and it  
235 is likely that it may be susceptible to radical attack (Lu et al. 2003). LPS layer and the phospholipid bilayer  
236 are made up of fatty acids, which may be also susceptible to radicals attack. The possibility of radicals to travel  
237 only very short distances and the presence of an intact membrane reduce the probability of the radical reaching  
238 intracellular components such as DNA, but once the radicals are generated in close proximity to the target  
239 molecules, they will be able to inflict injury directly (Dalrymple et al. 2010). On the other hand, two  $\cdot\text{OH}$   
240 radicals may recombine to form hydrogen peroxide, which may inactivate bacterial cells on a longer distance  
241 between the source of radicals and the target (Foster et al. 2011).

242

### 243 3.1.3 *S. typhimurium* mutagenicity during $\text{TiO}_2$ photocatalysis tests

244 The mutation frequencies were also evaluated following the  $\text{TiO}_2$  photocatalytic tests, and displayed a 42,  
245 1648, 32 fold increase compared to background level for a  $10^9$ ,  $10^8$  and  $10^7$  CFU  $\text{mL}^{-1}$  initial bacterial density,  
246 respectively (Fig. 2). The evolution of the mutation frequencies as a function of the treatment exposure time  
247 displayed biphasic aspects with an initial increase followed by a slow-down or a decrease as the exposure time  
248 increases. It is worth noting that the increased mutation frequencies are not associated to dramatic increases  
249 of the mutants counts; considering the fact that the emerging mutants are also subjected to an increase loss of  
250 cell viability, the apparent stability of the mutants counts probably result from an increased mutation frequency  
251 counterbalanced by an increased cell killing. If the levels of mutation reached were clearly different depending  
252 on the initial cell load (Fig. 2), statistical analyses demonstrated that the evolution of the mutation frequency  
253 (as a function of the exposure time) were similar for the  $10^8$  and  $10^7$  CFU  $\text{mL}^{-1}$  initial cell load (Supplementary  
254 section 4). This tends to show (i) that the treatment is in fact equally effective for these two initial cell loads  
255 in terms of dose-dependent effects, but (ii) the  $10^7$  CFU  $\text{mL}^{-1}$  suspension stops accumulating mutations earlier  
256 than the  $10^8$  CFU  $\text{mL}^{-1}$  probably because of a stronger killing effect.

257 The effect of different oxidants/disinfectants (namely chlorine, chlorine dioxide and ozone) on genotoxicity  
258 has been studied by different authors (Monarca et al. 2000; Mišić et al. 2011; Magdeburg et al. 2014), but no  
259 information is available in scientific literature (to authors' knowledge) on the effect of photocatalytic processes  
260 on the induction of mutants in *Salmonella* strains after treatment. Basically, *Salmonella* disinfection-induced  
261 mutagenicity has been mainly related to the formation of disinfection by-products. For example, Magdeburg  
262 et al. (2014) studied the effect of ozone, as tertiary treatment, in a pilot scale wastewater treatment. The Ames  
263 assay using *Salmonella typhimurium* strain YG7108 revealed an ozone-dose dependent mutagenicity increase

264 after wastewater ozonation, indicating the formation of alkylating mutagenic oxidation by-products. The  
265 impact of ozone treatment on genotoxic and acute toxic effects of tertiary treated municipal wastewater was  
266 investigated by Mišík et al. (2011). After ozone treatment, they observed a decrease of the mutagenic activity  
267 of the samples and the bactericidal effects were reduced by ozonation. The influence of disinfectants such as  
268 chlorine dioxide, ozone, peracetic acid and, UV radiation, on the formation of mutagenic compounds has been  
269 evaluated by Monarca et al. (2000). They evaluated the mutagenicity using the Ames test and all disinfectant  
270 treatments induced the formation of mutagenic compounds, particularly chemical treatment with ClO<sub>2</sub> or  
271 ozone, in contrast with physical treatment with UV-C lamp.

272 Despite the lack of work available in scientific literature concerning the effect of TiO<sub>2</sub> photocatalytic process  
273 on the formation of mutants in *Salmonella* strains, the possible role of hydroxyl radicals has been investigated  
274 (Kanno et al. 2012). De Kok et al. (1992) used electron spin resonance (ESR) spectroscopy to detect and  
275 identify oxygen species generated by fecapentaenes (potent genotoxins found in human feces) and investigated  
276 the influence of scavenging reactive oxygen species (dimethyl sulfoxide (DMSO), t-butyl alcohol, t-butyl  
277 hydroperoxide (TBOOH), 2,2,6,6-tetramethylpiperidine and 5,5-dimethyl-1-pyrroline-A'-oxide) on the  
278 mutagenicity of *Salmonella* strains including TA102. All hydroxyl radical scavengers significantly reduced  
279 the number of revertants (except for DMSO in combination with TBOOH), thus showing that hydroxyl radical  
280 could mediate mutagenicity of the *Salmonella* strains although the precise mechanisms did not appear clearly  
281 identified. In another study, hydrogen peroxide-induced mutagenicity in *Salmonella typhimurium* TA102 was  
282 assumed to be caused by hydroxyl radicals generated by iron ions closely associated with DNA, since iron  
283 chelators or hydroxyl radical scavengers (ascorbic acid or DMSO) exhibited effective anti-mutagenic effects  
284 (Grey and Adlercreutz, 2003).

285

## 286 **3.2 UV-C disinfection tests**

### 287 *3.2.1 S. typhimurium TA102 inactivation by UV-C disinfection tests*

288 UV-C irradiation tests were carried out in order to compare the results from TiO<sub>2</sub> photocatalytic process with  
289 a more conventional disinfection process. Figure 3 shows the evolution of cell counts and mutation frequencies  
290 as a function of UV energy. Control tests carried out in the dark (sample stored at room temperature for 4  
291 hours) did not show any change in bacterial cultivability (data not shown).

292

Figure 3

293

294

295 Whatever the initial cell load, a progressive loss of cultivability of strain TA102 was observed as the UV-dose  
296 was increased, which was confirmed by a Pearson correlation test (Supplementary section 2). For the highest  
297 initial cell load ( $10^9$  CFU mL<sup>-1</sup>), the total cell count dropped down by 9 log units and total inactivation was  
298 reached after about 45 min of UV exposure (Fig.3a), which correspond to a 30 mWs cm<sup>-2</sup> (45 min irradiation  
299 time) UV-C dose. As the initial bacterial density was decreased to  $10^8$  (Fig. 3b) and  $10^7$  (Fig. 3c) CFU mL<sup>-1</sup>,  
300 the total bacteria inactivation was achieved in 15 and 10 min, respectively while the corresponding UV-C  
301 doses were relatively close in both experiments (approximately 5-10 mWs cm<sup>-2</sup>). Statistically, the cell count  
302 abatements ( $\log(N/N_0)$ ) appeared similar in terms of dose-dependent decrease for the two lower initial cell  
303 loads (Supplementary section 5) although longer treatment are necessary to achieve a full inactivation of the  
304 higher initial cell load. The cell count abatement obtained for the  $10^9$  CFU mL<sup>-1</sup> suspension appeared to  
305 decrease at a significant lower pace (Supplementary Fig. S5) compare the two other suspensions, which  
306 probably reflect the shield effect exerted by bacteria when the cell density is too high. However, a direct  
307 dependence of initial concentration of microorganism and UV dose necessary to reach a full cell inactivation  
308 was expected. Its estimation was based on the averaged incident radiation energy over the reactor volume that  
309 is a dynamic function of the absorption coefficient, which itself depends dynamically on the concentration of  
310 active cells (Silva et al. 2013). UV-C disinfection relies on the sensitivity of the microorganism to UV  
311 radiation. This is unique to each microorganism and is determined by its ability to absorb at 200–280 nm  
312 (germicidal wavelength range), so inactivating their active cells through UV-induced damages such as the  
313 formation of pyrimidine dimers in their DNA. UV-induced damages disrupt the DNA structure, so that, if a  
314 critical number of dimers is formed, the DNA cannot replicate (Hignen et al. 2006).

315 At a first glimpse, the cell complete inactivation was faster in the UV-C disinfection experiments compared  
316 to photocatalytic disinfection experiments for all initial bacterial densities investigated (Fig.2). However,  
317 considering the energy engaged in both treatments, the photocatalytic process was more efficient than the UV-  
318 C process because a lower energy was required to achieve a total *S. typhimurium* inactivation (in the range 2  
319 - 20 mWs cm<sup>-2</sup>).

320

321 3.2.2 *S. typhimurium* mutagenicity during UV-C disinfection tests

322 The mutation frequencies, increased in a UV-C dose dependent manner to reach a maximum corresponding  
323 to a 21, 2181 and 26 fold increase compared to background level, for  $10^9$ ,  $10^8$  and  $10^7$  CFU mL<sup>-1</sup> initial  
324 bacterial density, respectively (Fig. 3). UV-C doses higher than 7.2, 2.4 and 0.5 mWs cm<sup>-2</sup> respectively,  
325 resulted in absence of detectable mutants, where the deleterious effect of the UV-C treatment ultimately  
326 dominates over the emergence of mutants (Fig.3). As for the photocatalytic treatment, the evolution of the  
327 mutation frequencies displayed a dose-dependent biphasic aspects with an initial increase followed by a slow-  
328 down/decrease for higher UV-C doses. Here again, statistical analysis demonstrated that the initial increase of  
329 the log(F/F<sub>0</sub>) ratio appeared to evolve at a lower pace for the  $10^9$  CFU mL<sup>-1</sup> cell suspension than the  $10^8$  and  
330 the  $10^7$  CFU mL<sup>-1</sup> ones (Supplementary section 5), which mean that different initial cell load are not equally  
331 sensitive as far as cell are numerous enough to exert a shield effect. UV radiation produces many types of  
332 photochemical alterations (e.g., in DNA, RNA, protein, membranes) but DNA remains the major target for  
333 the deleterious effects of UV radiation all together because of its large size, its efficient UV absorption, its  
334 low number of copies per cells, and finally because it is the support of genetic information (Grossweiner et al.  
335 2005). A large number of different types of damage are produced in DNA by UV irradiation however,  
336 mutagenic lesions principally result from the formation of pyrimidine dimers and pyrimidine adducts (Sinha  
337 and Häder 2002). UV-induced mutagenesis is a highly complex process involving different photoproducts and  
338 repair mechanisms that deal with them. Tate et al. (2006) characterized the damage of UV-C radiation in  
339 *Salmonella typhimurim* strain TA98. The damage was found primarily localized in the nucleic acids and it  
340 results from direct absorption of photons by the target molecules. According to the authors, the damage  
341 produced by UV-C was predominately in the form of pyrimidine dimers and 6-4 photoproducts resulting from  
342 the direct photon absorption by DNA. UV-induced mutations in *Salmonella* are relevant not only regarding  
343 lethality, but also because it may favor the appearance of some antibiotic resistances (Michael et al. 2006).  
344 With this respect, it is worth noting that in the case of UV-C disinfection tests carried out with  $10^7$  CFU mL<sup>-1</sup>,  
345 a one log increased titer of His<sup>+</sup> mutants was observed together with the increasing mutation frequency.  
346 Possibly in this setup, from 0 to 0.2 mWs cm<sup>-2</sup>, the appearance of mutants is not compensated by cell death as  
347 the mutation frequency increases. This was also observed but to a lesser extent with the other treatment.

348

#### 349 4. Conclusions

350 TiO<sub>2</sub> photocatalysis was compared with UV-A (control) and UV-C radiations both in terms of cell inactivation  
351 and appearance of mutants in *Salmonella typhimurium* TA102 dispersed in water. In the investigated  
352 conditions, the inactivation rate appeared faster in the UV-C radiation experiments (10 min for total  
353 inactivation with an initial density of 10<sup>7</sup> CFU mL<sup>-1</sup>) than the photocatalytic experiments (15 min). But  
354 photocatalytic process was more energy efficient because a lower energy was required (2 - 20 mWs cm<sup>-2</sup>,  
355 depending on initial bacterial density) compared to UV-C disinfection process (5 - 30 mWs cm<sup>-2</sup>). In most  
356 experiments, the appearance of mutants seemed to be counterbalanced by cell death, which results in an  
357 increasing mutation frequency with no increase of the His<sup>+</sup> mutant titers. In some case though, a significant  
358 increase of the His<sup>+</sup> mutant titers was observed before full inactivation. Possibly, in particular conditions  
359 where disinfection is incomplete, the selected process may pose a risk of releasing more mutants than untreated  
360 cell suspensions, with possible consequences regarding mutation-dependent acquisition of antibiotic  
361 resistances. Statistically, both the bacterial inactivation and the evolution of the mutation frequencies appeared  
362 directly dependent of initial concentration of microorganism and treatment dose, whatever the treatment, UV-  
363 C or photocatalysis respectively. This necessarily implies to carefully consider the cell density if the generation  
364 of mutants is to be prevented in disinfection setup.

365

366

#### 367 Acknowledgements

368 The support of University of Salerno through FARB2012 (Trattamento avanzato di acque reflue urbane  
369 mediante fotocatalisi: effetto sui batteri resistenti agli antibiotici) project funding is acknowledged. The  
370 authors would like also to acknowledge the financial support provided by COST-European Cooperation in  
371 Science and Technology, to the COST Action “TD0803: Detecting evolutionary hotspots of antibiotic  
372 resistances in Europe (DARE)” and COST Action “ES1403: New and emerging challenges and opportunities  
373 in wastewater reuse (NEREUS)”. CM wishes to thank the “Zone Atelier Moselle” (ZAM) for supporting his  
374 research on treatment processes and their effects. Disclaimer: The content of this article is the authors’

375 responsibility and neither COST nor any person acting on its behalf is responsible for the use, which might be  
376 made of the information contained in it.  
377  
378



379           **References**

- 380    Berney HU, Weilenmann A, Simonetti T (2006) Efficacy of solar disinfection of *Escherichia coli*,  
381    *Shigella flexneri*, *Salmonella* Typhimurium and *Vibrio cholerae*. J Appl Microbiol 101(4):828-836
- 382    Cho M, Chung H, Choi W, Yoon J, (2004) Linear correlation between inactivation of *E. coli* and OH  
383    radical concentration in TiO<sub>2</sub> photocatalytic disinfection. Water Res 38:1069–1077
- 384    Dalrymple OK, Stefanakos E, Trotz MA, Goswami DY (2010) A review of the mechanisms and  
385    modeling of photocatalytic disinfection. Appl Catalysis B: Environ 98:27–38
- 386    de Kok TM, van Maanen JM, Lankelma J, ten Hoor F, Kleinjans JC (1992) Electron spin resonance  
387    spectroscopy of oxygen radicals generated by synthetic fecapentaene-12 and reduction of fecapentaene  
388    mutagenicity to *Salmonella typhimurium* by hydroxyl radical scavenging. Carcinogenesis 13:1249–  
389    1255
- 390    Dunlop PSM, Ciavola M, Rizzo L, Byrne JA (2011) Inactivation and injury assessment of *Escherichia*  
391    *coli* during solar and photocatalytic disinfection in LDPE bags. Chemosphere 85:1160-1166
- 392    Fàbrega A, Vila J (2013) *Salmonella enterica* serovar Typhimurium skills to succeed in the host:  
393    virulence and regulation. Clin Microbiol Rev 26(2):308-341
- 394    Foster HA, Ditta IB, Varghese S, Steele A (2011) Photocatalytic disinfection using titanium dioxide:  
395    spectrum and mechanism of antimicrobial activity. Appl Microbiol Biotechnol. 90(6):1847-1868
- 396    Grossweiner LI, Jones LR, Grossweiner JB, Rogers BHG (2005) Photochemical Damage to Biological  
397    Systems. In *The Science of Phototherapy: an Introduction* (Ed Jones), Springer the Netherlands.
- 398    Gordon MA, Graham SM, Walsh AL, Wilson LK, Phiri A, Molyneux EM, et al. (2008) Epidemics of  
399    invasive *Salmonella enterica* serovar Enteritidis and *Salmonella enterica* serovar Typhimurium  
400    infection associated with multidrug resistance among adults and children in Malawi. Clin Infect Dis  
401    46:963-969
- 402    Grey CE, Adlercreutz P (2003) Ability of antioxidants to prevent oxidative mutations in *Salmonella*  
403    typhimurium TA102. Mutat Res 527:27–36
- 404    Haley BJ and Cole D (2009) Distribution, diversity, and seasonality of waterborne salmonellae in a  
405    rural watershed. Appl Environ Microb 75(5):1248-1255
- 406    Hignen WAM and Medema GJ (2006) Inactivation credit of UV radiation for viruses, bacteria and  
407    protozoan (oo)cysts in water: A review. Water Res 40(1):3-22

408 Kanno T, Nakamura K, Ikai H, Kikuchi K, Sasaki K, Niwano Y (2012) Literature review of the role of  
409 hydroxyl radicals in chemically induced mutagenicity and carcinogenicity for the risk assessment of a  
410 disinfection system utilizing photolysis of hydrogen peroxide. *J Clin Biochem Nutr* 51:9–14

411 Koivunen J and Heinonen-Tanski H (2005) Inactivation of enteric microorganisms with chemical  
412 disinfectants, UV radiation and combined chemical/UV treatments. *Water Res* 39(8):1519-1526

413 Levantesi C, Bonadonna L, Briancesco R, Grohmann E, Toze S, Tandoi V (2012) *Salmonella* in surface  
414 and drinking water: Occurrence and water-mediated transmission. *Food Res Internat* 45(2): 587-602

415 Levantesi C, La Mantia R, Masciopinto C, Uta Böckelmann C et al. (2010) Quantification of pathogenic  
416 microorganisms and microbial indicators in three wastewater reclamation and managed aquifer  
417 recharge facilities in Europe. *Sci Total Environ* 408(21):4923-4230

418 Li H, Bhaskara A, Megalis C, Tortorello ML (2012) Transcriptomic analysis of *Salmonella* desiccation  
419 resistance. *Foodborne Pathog Dis* 9:1143–1151

420 Long M, Wang J, Zhuang H, Zhang Y, Wu H, and Zhang J (2014) Performance and mechanism of  
421 standard nano-TiO<sub>2</sub> (P-25) in photocatalytic disinfection of foodborne microorganisms—*Salmonella*  
422 typhimurium and *Listeria monocytogenes*. *Food Control* 39(1):68–74

423 Lu Z-X, Zhou L, Zhang Z-L, Shi W-L, Xie Z-X, Xie H-Y, Pang D-W, Shen P (2003) Cell Damage  
424 Induced by Photocatalysis of TiO<sub>2</sub> Thin Films. *Langmuir* 19:8765-8768

425 Magdeburg A, Stalter D, Schlsener M, Ternes T, Oehlmann J (2014) Evaluating the efficiency of  
426 advanced wastewater treatment: target analysis of organic contaminants and (geno-)toxicity assessment  
427 tell a different story. *Water Res* 50(0):35-47

428 Majowicz SE, Musto J, Scallan E, Angulo FJ, Kirk M, O'Brien SJ, Jones TF, Fazil A, Hoekstra RM  
429 (2010) The global burden of nontyphoidal *Salmonella gastroenteritis*. *Clin Infect Dis* 50:882–889

430 Maron DM, Ames BN (1983) Revised methods for *Salmonella* mutagenicity test. *Mutat Res* 101: 173-  
431 215

432 Martinez-Urtaza J, Saco M, de Novoa J, Perez-Pineiro P, Peiteado J, Lozano-Leon A, Garcia-Martin O  
433 (2004) Influence of environmental factors and human activity on the presence of *Salmonella* serovars  
434 in a marine environment. *Appl Environ Microbiol* 70:2089–2097

435 Masarikova M, Manga I, Cizek A, Dolejska M, Oravcova V, Myskova P, Karpiskova R, Literak I  
436 (2016) *Salmonella enterica* resistant to antimicrobials in wastewater effluents and black-headed gulls  
437 in the Czech Republic, 2012. *Sci Total Environ* 542:102–107

438 McGuigan KG, Conroy RM, Mosler H-J, du Preez M, Ubomba-Jaswa E, Fernandez-Ibanez P (2012)  
439 Solar water disinfection (SODIS): A review from bench-top to roof-top. J Hazard Mater 235– 236:29–  
440 46

441 Michael GB, Butaye P, Cloeckeaert A, Schwarz S (2006) Genes and mutations conferring antimicrobial  
442 resistance in *Salmonella*: an update. Microbes Infect 8(7):1898-1914

443 Mišić M, Knasmueller S, Ferk F, Cichna-Markl M, Grummt T, Schaar H, Kreuzinger N (2011) Impact  
444 of ozonation on the genotoxic activity of tertiary treated municipalwastewatr. Water Res 45(12):3681-  
445 3691

446 Monarca S, Feretti D, Collivignarelli C, Guzzella G, Zerbini I, Bertanza G, Pedrazzani R (2000) The  
447 influence of different disinfectants on mutagenicity and toxicity of urban wastewater. Water Res  
448 34(17):4261-4269

449 Nutt JD, Li X, Woodward CL, Zabala-Diaz IB and Ricke SC (2003) Growth kinetics response of a  
450 *Salmonella* Typhimurium poultry marker strain to fresh produce extracts. Bioresource Technol 89:313-  
451 316

452 Oubrim N, Ennaji MM, Badri S, Cohen N (2012) Removal of Antibiotic-Resistant *Salmonella* in  
453 Sewage Water from Wastewater Treatment Plants in Settat and Soualem, Morocco. Eur J Sci Res  
454 68(4):565-573

455 Polo F, Figueras MJ, Inza I, Sala J, Fleisher JM, Guarro J (1999) Prevalence of *Salmonella* serotypes  
456 in environmental waters and their relationships with indicator organisms. A Van Leeuw 75:285–292

457 Polo-López MI, Castro-Alfárez M, Oller I, Fernández-Ibáñez P (2014) Assessment of solar photo-  
458 Fenton, photocatalysis, and H<sub>2</sub>O<sub>2</sub> for removal of phytopathogen fungi spores in synthetic and real  
459 effluents of urban wastewater. Chemi Eng J 257:122-130

460 Popoff M Y (2001) Antigenic formulas of the *Salmonella* serovars. WHO Collaborating Center for  
461 Reference and Research on Salmonella (8th ed). Institut Pasteur Paris, France.

462 Rahmani M, Peighambari S M, Svendsen C A, Cavaco L M, Agersø Y, Hendriksen RS (2013)  
463 Molecular clonality and antimicrobial resistance in *Salmonella enterica* serovars Enteritidis and Infantis  
464 from broilers in three Northern regions of Iran. BMC Vet Res 9:66

465 Rahmani BA, Wasfy MO, Maksoud MA, Hanna N, Dueger E, House B (2014) Multi-drug resistance  
466 and reduced susceptibility to ciprofloxacin among *Salmonella enterica* serovar Typhi isolates from the  
467 Middle East and Central Asia. New Microbes and New Infect 2(4):88-92

468 Rincon AG, Pulgarin C (2007) Fe<sup>3+</sup> and TiO<sub>2</sub> solar-light-assisted inactivation of *E. coli* at field scale  
469 – implications in solar disinfection at low temperature of large quantities of water. *Catal Today* 122:  
470 128–136.

471 Rizzo L (2011) Bioassays as a tool for evaluating advanced oxidation processes in water and wastewater  
472 treatment. *Water Res* 45:4311-4330

473 Rizzo L, Manaia C, Merlin C, Schwartz T, Dagot C, Ploy MC, Michael I, Fatta-Kassinos D (2013)  
474 Urban wastewater treatment plants as hotspots for antibiotic resistant bacteria and genes spread into the  
475 environment: A review. *Sci Total Environ* 447:345-360

476 Rizzo L, Ferro G, Manaia CM (2014a) Wastewater disinfection by solar heterogeneous photocatalysis:  
477 Effect on tetracycline resistant/sensitive enterococcus strains. *Global Nest Journal* 16: 455-462

478 Rizzo L, Della Sala A, Fiorentino A, Li Puma G (2014b) Disinfection of urban wastewater by solar  
479 driven and UV lamp - TiO<sub>2</sub> photocatalysis: Effect on a multi drug resistant *Escherichia coli* strain.  
480 *Water Res* 53:145-152

481 Robertson GP (2005) Functional and therapeutic significance of Akt deregulation in malignant  
482 melanoma. *Cancer Metast Rev* 24:273–285

483 Sciacca J, Rengifo-Herrera J, Wethe, Pulgarin C (2011) Solar disinfection of wild *Salmonella* sp. in  
484 natural water with a 18 L CPC photoreactor: Detrimental effect of non-sterile storage of treated water.  
485 *Sol Energy* 85:1399–1408

486 Sharma VK, Johnson N, Cizmas L, McDonald TJ, Kim H (2016). A review of the influence of treatment  
487 strategies on antibiotic resistant bacteria and antibiotic resistance genes. *Chemosphere* 150:702-714

488 Silva RC, Cardoso WM, Teixeira RSC, Albuquerque ÁH, Horn RV, Cavalcanti CM (2013) *Salmonella*  
489 *Gallinarum* virulence in experimentally infected Japanese quails (*Coturnix japonica*). *Braz J of Poult*  
490 *Science* 15(1):39-45

491 Sinha RP, Häder DP (2002) UV-induced DNA damage and repair: a review. *Photochem Photobiol Sci*  
492 1(4):225-236

493 Simonet J, Gantzer C (2006) Inactivation of poliovirus 1 and F-specific RNA phages and degradation  
494 of their genomes by UV irradiation at 254 nanometers. *Appl Environ Microbiol* 72(12):7671-7677

495 Tate P, Stannera A, Shieldsa K, Smithc S, Larcom L (2006) Blackberry extracts inhibit UV-induced  
496 mutagenesis in *Salmonella typhimurium* TA100. *Nutrition Research* 26:100–104

497 Wang J, Zhuan H, Hinton A Jr., Bowker B, Zhang J (2014) Photocatalytic disinfection of spoilage  
498 bacteria *Pseudomonas fluorescens* and *Micrococcus caseolyticus* by nano-TiO<sub>2</sub>. LWT - Food Science  
499 and Technology 59(2):1009–1017

500 Wéry N, Lhoutellier C, Ducray F, Delgenès JP & Godon JJ (2008) Behaviour of Pathogenic and  
501 Indicator Bacteria During Urban Wastewater Treatment and Sludge Composting, as Revealed By  
502 Quantitative PCR. Water Res 42:53-62

503

504 **Figure captions**

505 **Fig. 1** Control tests on TiO<sub>2</sub>/UV experiments: effect of UV-A radiation on the inactivation and the formation  
506 of mutants for three different initial cell loads of strain TA102: 10<sup>9</sup> (a), 10<sup>8</sup> (b) and 10<sup>7</sup> (c) CFU.mL<sup>-1</sup>. Error  
507 bars represent standard deviation from three independent experiments

508 **Fig. 2** Effect of TiO<sub>2</sub>/UV process on the inactivation and the formation of mutants for three different initial  
509 cell loads of strain TA102: 10<sup>9</sup> (a), 10<sup>8</sup> (b) and 10<sup>7</sup> (c) CFU.mL<sup>-1</sup>. Error bars represent standard deviation from  
510 three independent experiments

511 **Fig. 3** Effect of UV-C process on the inactivation and the formation of mutants for three different initial cell  
512 loads of strain TA102: 10<sup>9</sup> (a), 10<sup>8</sup> (b) and 10<sup>7</sup> (c) CFU.mL<sup>-1</sup>. Error bars represent standard deviation from  
513 three independent experiments

514

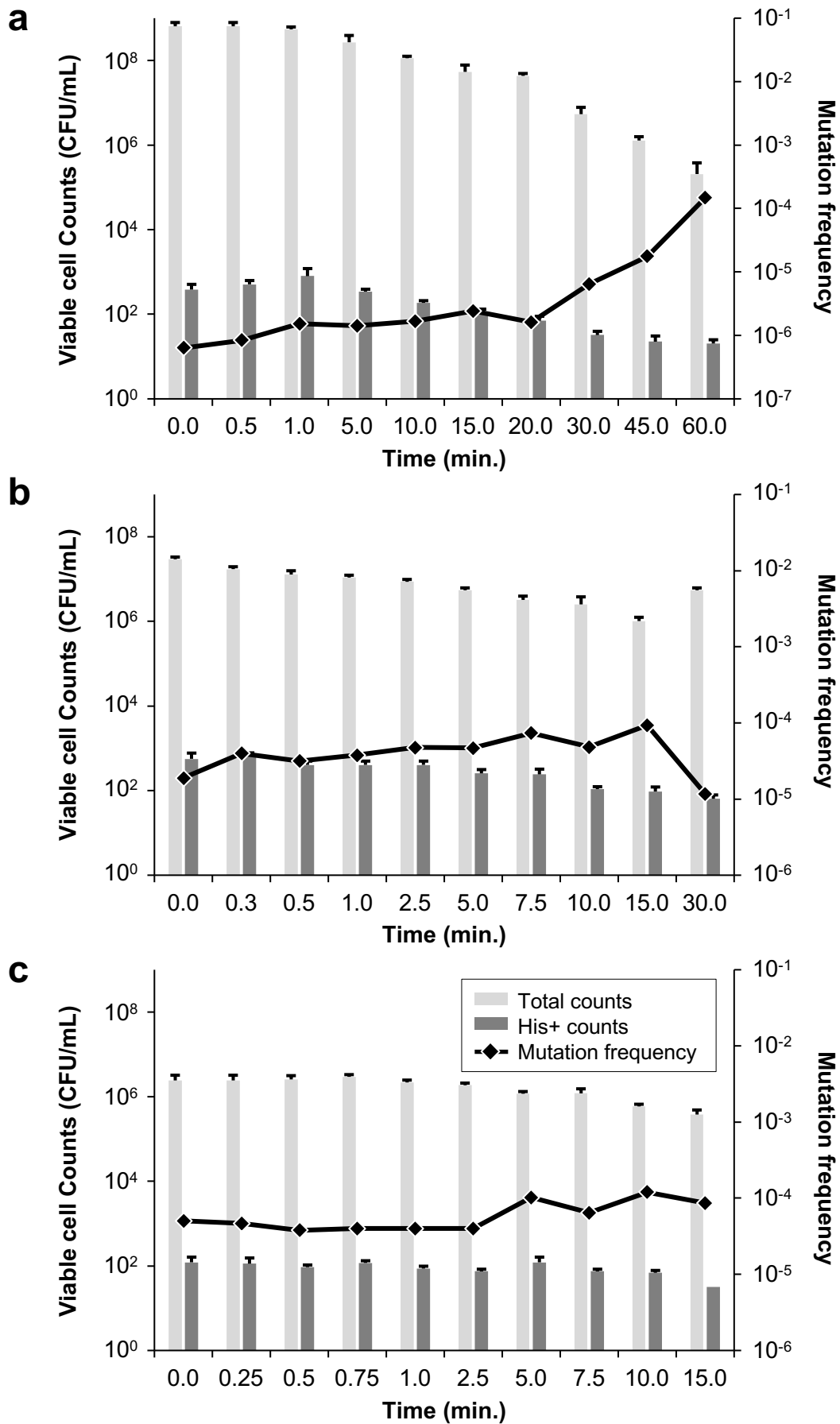


Figure 1

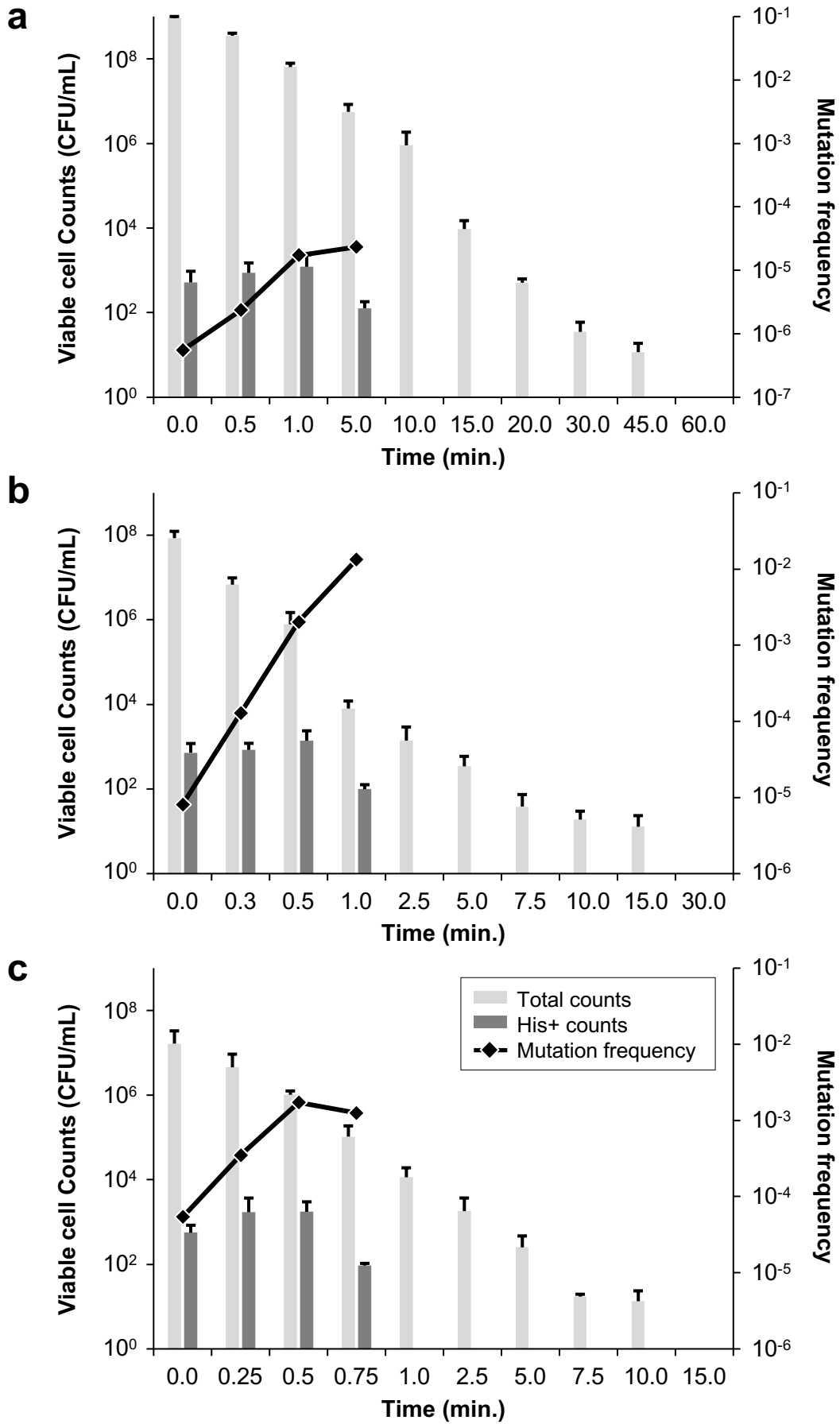


Figure 2



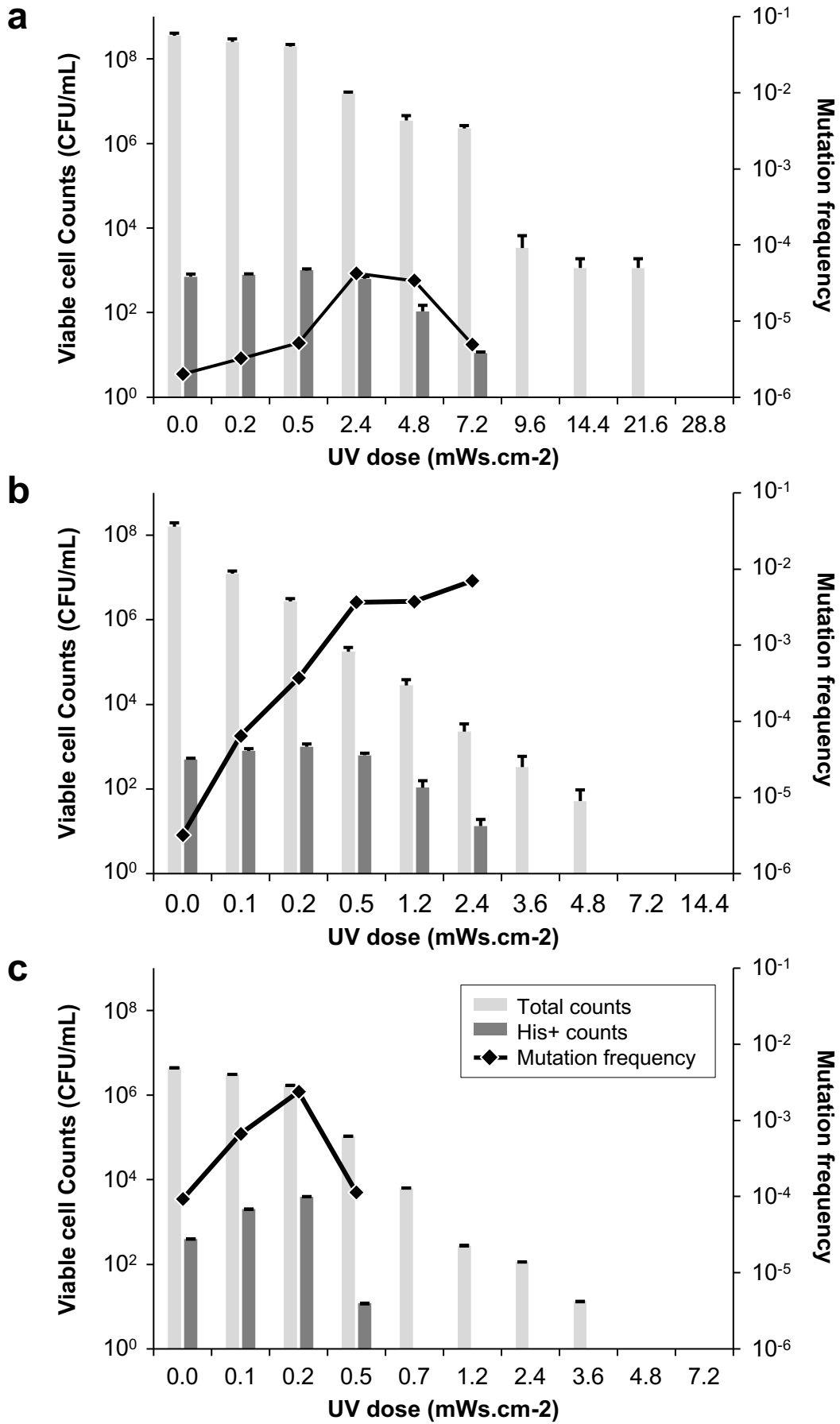


Figure 3

## Supplementary material

Comparing TiO<sub>2</sub> photocatalysis and UV-C radiation for inactivation and mutants formation of *Salmonella typhimurium* TA102

Antonino Fiorentino, Luigi Rizzo, H  l  ne Guilloteau, Xavier Bellanger, Christophe Merlin.

### Table of content:

1. Statistical analysis procedures
2. Dose-dependent effects of the treatments on bacterial viability
3. Statistical analysis of the UV-A treatment efficiency
  - 3.1. Regression analyses and trendline equations summaries
  - 3.2. Statistical comparison of the treatment efficiency as a function of the cell load
4. Statistical analysis of the UV-A + TiO<sub>2</sub> treatment efficiency
  - 4.1. Regression analyses and trendline equations summaries
  - 4.2. Statistical comparison of the treatment efficiency as a function of the cell load
5. Statistical analysis of the UV-C treatment efficiency
  - 5.1. Regression analyses and trendline equations summaries
  - 5.2. Statistical comparison of the treatment efficiency as a function of the cell load
6. Statistical comparison of the UV-A and UV-A + TiO<sub>2</sub> treatments

## 1. Statistical analysis procedures

The correlations between the bacterial mortality ( $\log(N/N_0)$ ) and the duration of the treatments, or the doses received, were assessed using the Pearson's test. Then, regression data analyses were performed on log-transformed data:  $\log(N/N_0)$  for the total cell counts and  $\log(F/F_0)$  for the frequencies of mutation. The effects of both the treatment and the initial bacterial cell load were analyzed using a Fisher F-test and a Student T-test. The Fisher F-test was used to test data for homogeneity of variances. Thereafter, once homogeneity was verified, a Student T-test was further used to compare the trends (slopes) of linear regressions. A statistical difference revealed by a Student T-test, combined to the comparison of regression trend-lines (slopes) allowed determining whether a given treatment or condition had stronger effects than another one.

## 2. Dose-dependent effects of the treatments on bacterial viability

The dose-dependent effect of each treatment (UV-C, UV-A, and UV-A + TiO<sub>2</sub>) on the bacterial viability (total cell count) was evaluated using a Pearson correlation test. For all conditions, the cell count abatements appeared statistically correlated to the treatment dose whatever the initial cell load (Table S1). Data were further analyzed to evaluate the statistical significance of the initial cell load and to compare treatments where possible.

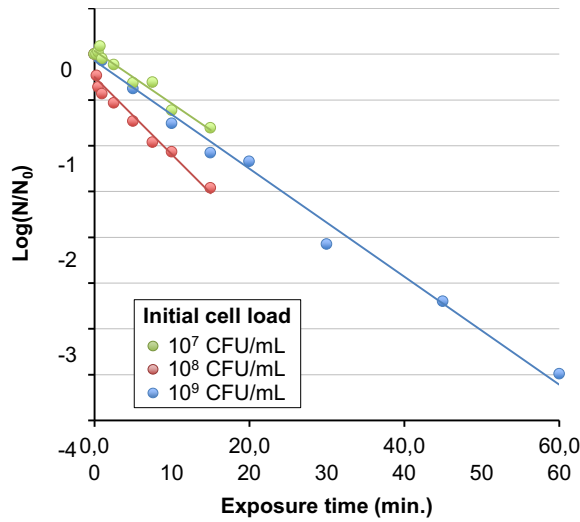
**Table S1:** Correlation between viable cell counts ( $\log(\text{CFU/mL})$ ) and the treatment dose (UV-C)/treatment duration (UV-A  $\pm$  TiO<sub>2</sub>) for the three different initial cell loads. The table provides "Pearson correlation coefficient" (PCC) and p-values (between parentheses).

Initial cell loads / treatment	10 <sup>9</sup> CFU/mL	10 <sup>8</sup> CFU/mL	10 <sup>7</sup> CFU/mL
UV-C	-0.957 (1.5 × 10 <sup>-5</sup> )	-0.840 (2.0 × 10 <sup>-3</sup> )	-0.876 (8.9 × 10 <sup>-4</sup> )
UV-A	-0.933 (7.9 × 10 <sup>-5</sup> )	-0.750 (1.2 × 10 <sup>-2</sup> )	-0.900 (3.8 × 10 <sup>-4</sup> )
UV-A + TiO <sub>2</sub>	-0.988 (1.0 × 10 <sup>-7</sup> )	-0.976 (1.3 × 10 <sup>-6</sup> )	-0.981 (5.2 × 10 <sup>-7</sup> )

### 3. Statistical analysis of the UV-A treatment efficiency

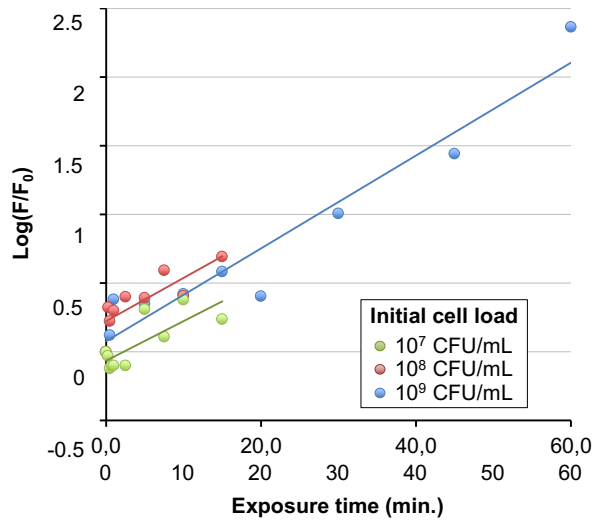
#### 3.1. Regression analyses and trendline equations summaries

**Fig. S1: Total viable cell counts abatements**



Initial cell load	10 <sup>9</sup> CFU/mL	10 <sup>8</sup> CFU/mL	10 <sup>7</sup> CFU/mL
Slope	-0.059	-0.085	-0.058
r <sup>2</sup>	0.991	0.942	0.964

**Fig. S2: Evolution of mutation frequencies**



Initial cell load	10 <sup>9</sup> CFU/mL	10 <sup>8</sup> CFU/mL	10 <sup>7</sup> CFU/mL
Slope	0.034	0.031	0.029
r <sup>2</sup>	0.933	0.674	0.609

#### 3.2. Statistical comparison of the treatment efficiency as a function of the cell load

At a first glimpse, the cell count abatement profiles (Fig. S1) and the evolution of the frequencies profiles (Fig. S2) for the UV-A treatment appeared relatively close to each other whatever the initial cell loads. This similarity was further confirmed by Student T-tests, whenever the comparison was authorized by Fisher F-tests (Tables S2 and S3).

**Table S2: Comparison of total cell counts abatements for the UV-A treatment.**

Initial cell load	10 <sup>9</sup> CFU/mL	10 <sup>8</sup> CFU/mL	10 <sup>7</sup> CFU/mL
10 <sup>9</sup> CFU/mL		≈	ND
10 <sup>8</sup> CFU/mL			ND
10 <sup>7</sup> CFU/mL			

**Table S3: Comparison of the evolutions of mutation frequencies for the UV-A treatment.**

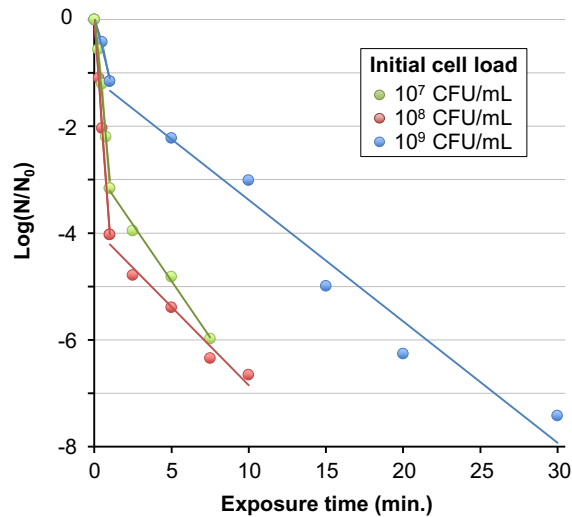
Initial cell load	10 <sup>9</sup> CFU/mL	10 <sup>8</sup> CFU/mL	10 <sup>7</sup> CFU/mL
10 <sup>9</sup> CFU/mL		≈	≈
10 <sup>8</sup> CFU/mL			≈
10 <sup>7</sup> CFU/mL			

**NA** : Not applicable (not enough data in the regression curve (2 points) to authorize a statistical comparison); **ND** : Not determined (variances not homogenous according to a Fisher F-test); **≠** : the trends (slopes) are significantly different ( $p > 0.05$ ); **≈** : the trends (slopes) are statistically similar ( $p \leq 0.05$ ).

#### 4. Statistical analysis of the UV-A + TiO<sub>2</sub> treatment efficiency

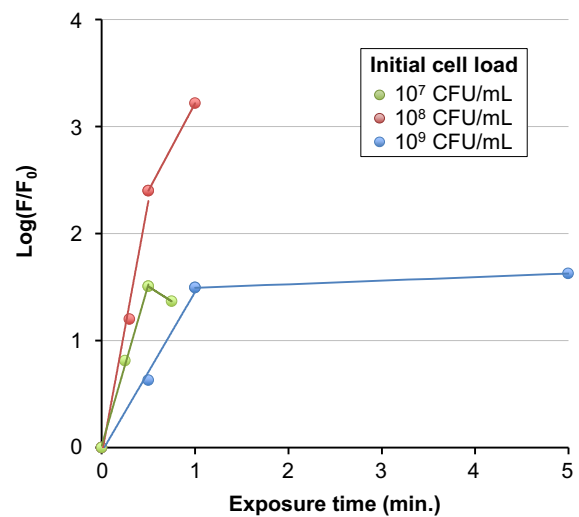
##### 4.1. Regression analyses and trendline equations summaries

**Fig. S3: Total viable cell counts abatements**



Initial cell load	10 <sup>9</sup> CFU/mL		10 <sup>8</sup> CFU/mL		10 <sup>7</sup> CFU/mL	
	part 1	part 2	part 1	part 2	part 1	part 2
Curves	part 1	part 2	part 1	part 2	part 1	part 2
Slope	-1.160	-0.227	-4.062	-0.293	-3.182	-0.422
r <sup>2</sup>	0.976	0.966	0.999	0.970	0.984	0.995

**Fig. S4: Evolution of the mutation frequencies**



Initial cell load	10 <sup>9</sup> CFU/mL		10 <sup>8</sup> CFU/mL		10 <sup>7</sup> CFU/mL	
	part 1	part 2	part 1	part 2	part 1	part 2
Curves	part 1	part 2	part 1	part 2	part 1	part 2
Slope	1.494	0.033	4.737	1.634	3.011	-0.553
r <sup>2</sup>	0.992	1.000	0.987	1.000	0.998	1.000

##### 4.2. Statistical comparison of the treatment efficiency as a function of the cell load

Both, the cell count abatement profiles (Fig. S3) and the evolution of the mutation frequencies profiles (Fig. S4) obtained for the UV-A+TiO<sub>2</sub> treatment tend to display a biphasic aspect with a trend linked to the initial cell loads. The biphasic aspects of the curves could be confirmed statistically by comparing the different parts of a same curve. When statistical comparisons were authorized by the Fisher F-test, the Student T-test showed that the treatment-dependent cell killing is significantly more reduced as the initial cell load increases (Fig. S3 and Table S2). Similarly, the analysis of the first part of the mutation frequency evolution curves, show that for an initial cell load of 10<sup>9</sup> CFU/mL, the time-dependent increase of the mutation frequency is significantly lower than for the two other cell concentrations (Fig. S4 and Table S3).

**Table S2:** Comparison of total cell counts abatements for the UV-A+TiO<sub>2</sub> treatment.

Initial cell load / curve part	10 <sup>9</sup> CFU/mL		10 <sup>8</sup> CFU/mL		10 <sup>7</sup> CFU/mL	
	part 1	part 2	part 1	part 2	part 1	part 2
10 <sup>9</sup> CFU/mL part 1		ND	≠		≠	
10 <sup>9</sup> CFU/mL part 2			ND	≈		ND
10 <sup>8</sup> CFU/mL part 1				≠	≠	
10 <sup>8</sup> CFU/mL part 2						≠
10 <sup>7</sup> CFU/mL part 1						≠
10 <sup>7</sup> CFU/mL part 2						

**Table S3:** Comparison of the evolutions of mutation frequencies for the UV-A+TiO<sub>2</sub> treatment.

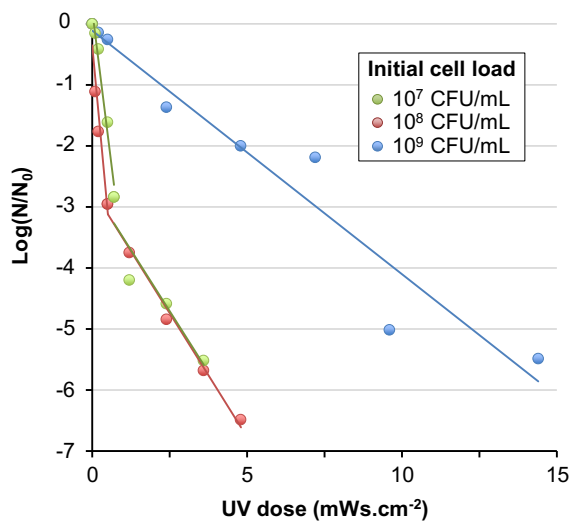
Initial cell load / curve part	10 <sup>9</sup> CFU/mL		10 <sup>8</sup> CFU/mL		10 <sup>7</sup> CFU/mL	
	part 1	part 2	part 1	part 2	part 1	part 2
10 <sup>9</sup> CFU/mL part 1		NA	≠		≠	
10 <sup>9</sup> CFU/mL part 2				NA		NA
10 <sup>8</sup> CFU/mL part 1				NA	≈	
10 <sup>8</sup> CFU/mL part 2						NA
10 <sup>7</sup> CFU/mL part 1						NA
10 <sup>7</sup> CFU/mL part 2						

**NA** : Not applicable (not enough data in the regression curve (2 points) to authorize a statistical comparison); **ND** : Not determined (variances not homogenous according to a Fisher F-test); **≠** : the trends (slopes) are significantly different ( $p > 0.05$ ); **≈** : the trends (slopes) are statistically similar ( $p \leq 0.05$ ).

## 5. Statistical analysis of the UV-C treatment efficiency

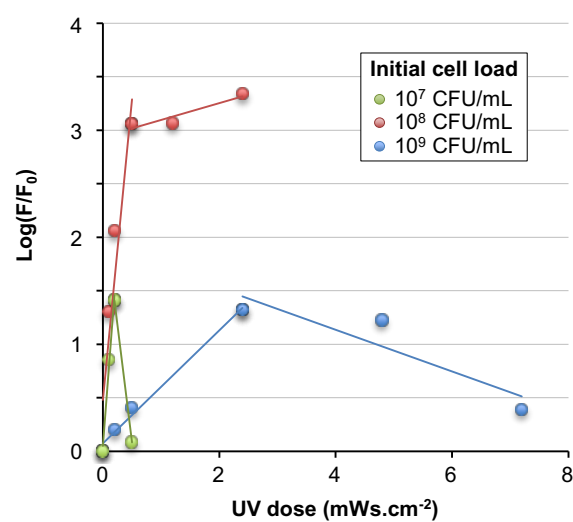
### 5.1. Regression analyses and trendline equations summaries

**Fig. S5: Total viable cell counts abatements**



Initial cell load	10 <sup>9</sup> CFU/mL		10 <sup>8</sup> CFU/mL		10 <sup>7</sup> CFU/mL	
	part 1	part 2	part 1	part 2	part 1	part 2
Curves	part 1	part 2	part 1	part 2	part 1	part 2
Slope	-0.399	-	-5.539	-0.811	-4.080	-0.800
r <sup>2</sup>	0.937	-	0.937	0.990	0.971	0.872

**Fig. S6: Evolution of the mutation frequencies**



Initial cell load	10 <sup>9</sup> CFU/mL		10 <sup>8</sup> CFU/mL		10 <sup>7</sup> CFU/mL	
	part 1	part 2	part 1	part 2	part 1	part 2
Curves	part 1	part 2	part 1	part 2	part 1	part 2
Slope	0.527	-0.195	5.618	0.157	7.048	-4.419
r <sup>2</sup>	0.989	0.828	0.887	0.888	0.985	1.000

### 5.2. Statistical comparison of the treatment efficiency as a function of the cell load

With the UV treatment, the biphasic aspect of the cell count abatement curves were solely observed for the initial cell loads of 10<sup>7</sup> and 10<sup>8</sup> CFU/mL (Fig. S5). When statistical comparison was authorized by the Fisher F-test, Student T-tests showed that for these two initial cell loads (i) the abatement curves are statistically similar and (ii) that the treatment is relatively more efficient than for an initial cell load of 10<sup>9</sup> CFU/mL (Fig. S5 and Table S4). Concerning the mutation frequencies profiles, the lack

of analysable datapoints (valid Fisher tests and/or enough datapoints on the trend line) authorized comparisons in a limited number of cases, mainly the first part of the curves for the two extreme initial cell loads. In such cases the Student T-test demonstrated that mutation frequencies increased faster as the initial cell load is smaller (Fig. S6 and Table S5).

**Table S4:** Comparison of total cell counts abatements for the UV-C treatment.

Initial cell load / curve part		10 <sup>9</sup> CFU/mL		10 <sup>8</sup> CFU/mL		10 <sup>7</sup> CFU/mL	
		part 1		part 1	part 2	part 1	part 2
10 <sup>9</sup> CFU/mL	part 1			≠	ND	ND	≈
	part 2						
10 <sup>8</sup> CFU/mL	part 1				≠	≈	NA
	part 2					NA	≈
10 <sup>7</sup> CFU/mL	part 1						≠
	part 2						

**Table S5:** Comparison of the evolutions of mutation frequencies for the UV-C treatment.

Initial cell load / curve part		10 <sup>9</sup> CFU/mL		10 <sup>8</sup> CFU/mL		10 <sup>7</sup> CFU/mL	
		part 1	part 2	part 1	part 2	part 1	part 2
10 <sup>9</sup> CFU/mL	part 1		≠	ND		≠	
	part 2				≈		NA
10 <sup>8</sup> CFU/mL	part 1				≠	ND	
	part 2						NA
10 <sup>7</sup> CFU/mL	part 1						NA
	part 2						

**NA** : Not applicable (not enough data in the regression curve (2 points) to authorize a statistical comparison); **ND** : Not determined (variances not homogenous according to a Fisher F-test); **≠** : the trends (slopes) are significantly different ( $p > 0.05$ ); **≈** : the trends (slopes) are statistically similar ( $p \leq 0.05$ ).

## 6. Statistical comparison of the UV-A and UV-A + TiO<sub>2</sub> treatments

UV-A and UV-A/TiO<sub>2</sub> treatments, which were carried out in the same conditions, were compared using Student T-tests. Whenever it was authorized by Fisher F-tests, the comparisons of the cell count abatements showed that (i) UV-A and UV-A+TiO<sub>2</sub> treatments are significantly different for a given initial cell load (Table S8), and (ii) with a stronger effect of the photocatalytic treatment according to the trends (slopes) of the linear regressions (Fig. S1, Fig. S3). The same tendencies were observed for the evolution of the mutation frequencies although the statistical comparison were authorized (Fisher F-test) for the two higher initial cell loads only (Table S7, Fig. S2, Fig. S4).

**Table S6:** Comparison of total cell counts abatements for the UV-A and UV-A + TiO<sub>2</sub> treatments.

Initial cell load and treatment	10 <sup>9</sup> CFU/mL UV-A + TiO <sub>2</sub>		10 <sup>8</sup> CFU/mL UV-A + TiO <sub>2</sub>		10 <sup>7</sup> CFU/mL UV-A + TiO <sub>2</sub>	
	part 1	part 2	part 1	part 2	part 1	part 2
10 <sup>9</sup> CFU/mL UV-A	≠	ND				
10 <sup>8</sup> CFU/mL UV-A			≠	≠		
10 <sup>7</sup> CFU/mL UV-A					ND	≠

**Table S7:** Comparison of the evolutions of mutation frequencies for the UV-A and UV-A + TiO<sub>2</sub> treatments.

Initial cell load and treatment	10 <sup>9</sup> CFU/mL UV-A + TiO <sub>2</sub>	10 <sup>8</sup> CFU/mL UV-A + TiO <sub>2</sub>	10 <sup>7</sup> CFU/mL UV-A + TiO <sub>2</sub>
	part 1	part 1	part 1
10 <sup>9</sup> CFU/mL UV-A	≠		
10 <sup>8</sup> CFU/mL UV-A		≠	
10 <sup>7</sup> CFU/mL UV-A			ND

**NA** : Not applicable (not enough data in the regression curve (2 points) to authorize a statistical comparison); **ND** : Not determined (variances not homogenous according to a Fisher F-test); **≠** : the trends (slopes) are significantly different ( $p > 0.05$ ); **≈** : the trends (slopes) are statistically similar ( $p \leq 0.05$ ).